

Preparation of an Aminated Bagasse Fiber and Its Mercury Adsorption Behavior

Nianfang Ma,¹ Shuixia Chen,^{1,2} Xilian Liu,¹ Ying Yang¹

¹PCFM Lab, OFCM Institute, School of Chemistry and Chemical Engineering, Sun Yat-Sen University, Guangzhou 510275, People's Republic of China

²Materials Science Institute, Sun Yat-Sen University, Guangzhou 510275, People's Republic of China

Received 8 December 2009; accepted 27 January 2010

DOI 10.1002/app.32174

Published online 27 April 2010 in Wiley InterScience (www.interscience.wiley.com).

ABSTRACT: An aminated bagasse (AB) with high-adsorption capacity for mercury ions was prepared by grafting copolymerization of acrylonitrile onto sugarcane bagasse, followed by aminating with chelating molecule diethylenetriamine. Effects of grafting conditions such as irradiation dosage, acrylonitrile concentration, and solvents on the grafting yield were investigated. The adsorption performance for mercury ions were evaluated by batch adsorption experiments and kinetic experiments. The results show that AB is effective for the removal of mercury over a wide range of pH > 5. Adsorption isotherms of mercury ions on the modified bagasse can be

well described by Langmuir equation. The equilibrium adsorption amount could be as high as 917.4 mg/g, and the removal percent of mercury ions can achieve 99%. The kinetic adsorption results indicate that AB could remove 80% of mercury ions in 2 h and 24 more hours are needed to achieve adsorption equilibrium. Regeneration experiments show that the adsorption capacity of recycled AB still can reach the level of 96% after four cycles. © 2010 Wiley Periodicals, Inc. *J Appl Polym Sci* 117: 2854–2861, 2010

Key words: sugarcane bagasse; amine group; mercury adsorption; chemical modification; irradiation grafting

INTRODUCTION

Toxic heavy metal contamination has aroused extensively concern nowadays, while disposition of the contaminated water is expensive and still a challenge due to very low discharge concentrations established by current regulations.^{1,2} Mercury is considered to be one of the most toxic heavy metals and possess serious threat to human life and natural environment,^{3,4} high-concentration of mercury even causes impairment of pulmonary and kidney function, chest pain, and dyspnoea.⁵ The permitted discharge limit of wastewater for total mercury is 10 µg/L.⁶ So to remove mercury ions in industrial wastewater prior to discharge became a top priority.

Adsorption treatment has found to be one of the most effective techniques that have been successfully employed for mercury removal from wastewater.^{7,8} Various adsorbents have been proposed for removing mercury and have been reviewed by Manohar et al.⁹ However, the high costs of the adsorbents limited its use, more importantly, they are not efficient when the mercury ions concentration is low.¹⁰ Therefore, it is very necessary to explore a low-cost material that has a good effect on the absorption of mercury.

Bagasse, an agriculture byproduct, has been extensively studied for heavy metal ions removal from aqueous solution, owing to its economic, nontoxic, renewable, biodegradable, and modifiable characteristics.^{11–14} It is a complex material containing lignin and cellulose as major constituents. The inexpensive eco-friendly bagasse has been prepared as activated carbons or by chemical modification into ion exchange adsorbents for heavy metal ions removal.^{15–19} As the adsorption capacity of raw bagasse for mercury is poor, modification of bagasse is a way to make up the disadvantage by introducing some chelating groups that possess strong affinity toward mercury.

The amino group is particularly effective in adsorption or removal of heavy metal ions from aqueous solution.²⁰ We are interested in the performance of their strong affinity toward mercury.²¹

Correspondence to: S. Chen (cescsx@mail.sysu.edu.cn).

Contract grant sponsor: Key Program of Science and Technology of Guangdong Province; contract grant number: 7117638.

Contract grant sponsor: Ph.D. Programs Foundation of Ministry of Education of China; contract grant number: 200805580007.

Contract grant sponsor: Science and Technology Project of Guangdong Province; contract grant number: 2008B010600039.

In the present investigation, amino groups were introduced to an aminated bagasse (AB) by amination of acrylonitrile grafted on the bagasse. The preparation conditions, structure, adsorption behaviors, and regeneration of AB for mercury were extensively studied.

EXPERIMENTAL

Materials and reagents

All reagents were of analytical grade if not specified and all solutions were prepared with deionized water. Glasswares used were repeatedly washed with HNO₃ and rinsed with deionized water. Sugarcane bagasse was obtained from a local sugar factory (Guangzhou, China). It was ground and screened to prepare 30 mesh size particles (around 600 μm), then the ground bagasse was dried in a vacuum oven for 24 h at 50°C. Diethylenetriamine (DETA) and mercury(II) chloride (HgCl₂·2H₂O) were purchased from Sigma-Aldrich. Nitric acid (HNO₃, top grade pure), sulfuric acid (H₂SO₄, top grade pure), acrylonitrile (AN), dimethylformamide (DMF), acetone, tetrahydrofuran (THF), chloroform, and aluminum chloride (AlCl₃·6H₂O) were used as received.

The reference and working solutions were diluted daily from stock mercury solution (2000 mg/L). Tin(II) chloride (SnCl₂) (10%, w/v) used as reducing agent was prepared by dissolving SnCl₂·2H₂O in 0.5M H₂SO₄. The pH was adjusted with the following buffer solutions: HNO₃ for pH 1.0; H₂C₂O₄/NaHC₂O₄ for pH 2.0 and 3.0; CH₃COONa/CH₃COOH for pH 4.0–6.0; Na₂HPO₄/NaH₂PO₄ for pH 7.0; Na₂B₄O₇/NaOH for pH 8.0–11; and NaOH for pH 12–13.

Preparation of AB

Pretreatment of sugarcane bagasse

The pretreatment of bagasse is an adaptation to a published procedure,²² first, the sugarcane bagasse was washed with deionized water under stirring at 80°C for 2 h and dried at 60°C. Second, the resulting bagasse was delignified with sodium chlorite at pH 4 (adjusted with 10% CH₃COOH), 75°C for 2 h, then washed with deionized water and 95% ethanol, and dried at 60°C for 24 h. Finally, the obtained bagasse was extracted with 10% NaOH at 20°C for 10 h to remove hemicelluloses, and then it was washed with distilled water, 95% ethanol sequentially, and dried in an oven at 50°C for 24 h.

Modification of sugarcane bagasse

A certain bath ratios of pretreated bagasse and AN were sealed in an ampoule and subjected to γ-rays

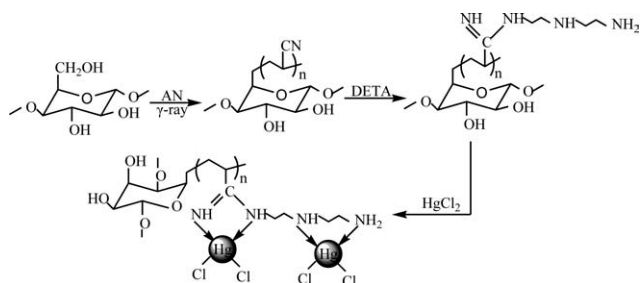


Figure 1 Synthesis chart of AB and the possible bind mode of AB with HgCl₂.

irradiation in the absence of air for a certain time. The dose rate of radiation was 0.837 KGy/h. After irradiation, the grafted bagasse was extracted in a Soxhlet apparatus with DMF to remove the residual monomer and homopolymer. The obtained bagasse grafted AN (bagasse-AN) were dried in a vacuum oven at 50°C for 48 h and then weighed. The degree of grafting (G%) is obtained according to the following formula:

$$G\% = \frac{W_g - W_o}{W_o} \times 100 \quad (1)$$

where W_o and W_g are the weight of the bagasse and bagasse-AN, respectively.

Then, the bagasse-AN, 100 mL of DETA and 4.0 g of AlCl₃·6H₂O were added into a 250 mL flask and suspended by a stirrer. The excess DETA was used as both the solvent and reactant. The reaction was carried out at 120°C for 3 h. Then the obtained AB was washed with deionized water and 95% ethanol, and dried at 50°C under vacuum. The synthesis chart of AB and the bind mode with mercury maybe depicted as in Figure 1.

Structure measurements and thermal analysis

Infrared spectra were obtained with FTIR analyzer (Nicolet/Nexus 670). FTIR-ATR measurements were carried out at a range of 4000–650 cm⁻¹, equipped with a continuum microscope and ATR objective. Elemental analyzer (Vario EL) was used for elemental analysis.

Thermogravimetry (TG) analyzer (NetzschTG-20) was used for thermal stability characterizations of all samples. The thermograms were obtained under a nitrogen atmosphere at a uniform heating rate of 20°C/min from ambient temperature to 600°C.

Batch procedure

The samples (0.05 g of each) were added into 100 mL of the mercury solutions in the 200 mL Erlenmeyer flasks and adjusted to desired pH. Then the

flasks were sealed and shaken for 24 h at 30°C. The effect of pH value on the mercury adsorption was studied at pH 1.0–13.0, by using 100 mg/L of the mercury solution. The pH value of the solutions was adjusted with buffer solutions.

For the optimized condition, the equilibrium adsorption experiments were conducted at pH 5.0 in batch modes. The effect of the initial concentration of the metal ions on the adsorption capacity was investigated in the range of 20–1000 mg/L as well as the adsorption time was investigated in the range of 0–24 h. Buffer solution is used to control the pH. The adsorption amount was calculated as follows:

$$Q = V(C_0 - C_e)/w \quad (2)$$

where Q is the adsorption amount (mg/g); w , the weight of the AB (g); V , the volume of solution (L); and C_0 and C_e are the concentrations (mg/L) of mercury ions before and after adsorption, respectively.

Adsorption kinetics

Kinetic experiments at different initial concentrations were performed in a batch mode. Initial concentrations of mercury solutions were set at 1, 10, and 100 mg/L at pH 5. Samples of the flask solution were taken out at certain intervals for analyses of the mercury concentrations.

Desorption

Desorption experiments are conducted to investigate its regeneration. Four different desorption solution (1M HCl, 5M HCl, 3M HCl + 0.5%CS(NH₂)₂, 3M HCl + 2%CS(NH₂)₂ and 5M HNO₃) were tried. After adsorption experiments, the mercury-loaded AB is separated and washed with distilled water to remove unadsorbed mercury ions, and dried at 60°C for 6 h. Then agitated with desorption solution to desorb mercury ions adsorbed by AB. The adsorption and regeneration cycles were repeated four times.

RESULTS AND DISCUSSION

Effects of reaction conditions on grafting yield of bagasse-AN

Factors that affect the grafting yield such as irradiating dosage, concentration of AN (v/v) %, and solvents are taken into consideration. Figure 2 shows the effect of monomer concentration and irradiation dose on the grafting degree of bagasse-AN. It can be clearly seen that the grafting degree is increasing with the monomer concentration, which can be explained by the diffusion theory. At the same irra-

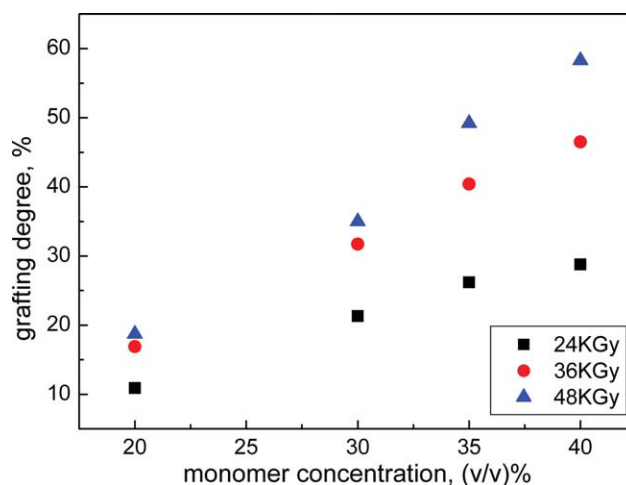


Figure 2 The effect of monomer concentration and irradiation dosage on the grafting yield of bagasse-AN. [Color figure can be viewed in the online issue, which is available at www.interscience.wiley.com.]

diation dosage, the active site on the bagasse would be the same, while the monomer diffused to graft onto the surface of bagasse increased with the monomer concentration increasing, thereby the grafting degree increased. On the other hand, the probability of homopolymerization of monomer also largely increased with the monomer concentration increasing, which decreased both the amount of monomer diffusing forward active site and the monomer diffusion rate resulting from the increased viscosity of the reactive system. The two factors lead to the decline of contact probability of monomer and active sites. Considering the grafting degree and the post-processing of removing homopolymer from bagasse-AN, 35% (v/v) of the monomer concentration would be most suitable.

The effect of irradiation dose on the grafting degree is similar to that of monomer concentration. As the irradiation dose increased, the active sites increased, consequently the monomer diffusing rate enhanced. Meanwhile, the homopolymerization was also largely increased with the irradiation dosage increased, whereas the homopolymerization and grafting copolymerization is a pair of competitive reaction. Besides, the higher irradiation dosage would bring more damage to bagasse. From a practical point of view, the irradiation dosage of 48KGy was chosen to prepare bagasse-AN for further experiment.

Figure 3 is the comparison of grafting degree of AN on bagasse in different solvent media. Four different solvents were chosen for investigating the effect of solvent polar on grafting degree. It is found that polar solvent DMF obtained the highest grafting degree and the lower polar solvent chloroform got the lowest. It can be interpreted as the following mechanism: when the polar solvent subject to

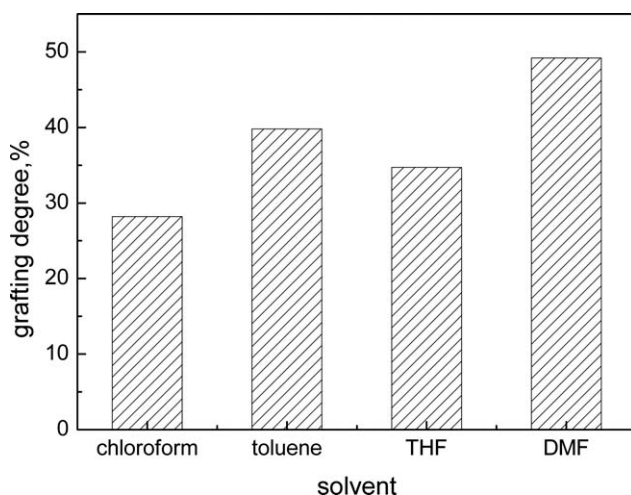


Figure 3 The effect of solvents on the grafting yield of bagasse-AN.

irradiation, a large amount of unstable H atoms would be generated, which will produce new active sites that can be used to initiate grafting copolymerization.²³

Structure of the modified bagasse

Figure 4 shows the IR spectra of bagasse, bagasse-AN, and AB. The peaks for the bagasse can be assigned as follows: 3373 cm^{-1} and 2901 cm^{-1} (γ_{OH} of bagasse and $\gamma_{\text{C-H}}$ of CH, CH_2 groups in alkyl and aromatic), 1042 cm^{-1} ($\gamma_{\text{C-O}}$), 1166 cm^{-1} ($\gamma_{\text{asC-O}}$), where γ represents a stretching vibration, γ_{as} represents a antisymmetric stretching vibration.²⁴ Comparing with the spectrum of the bagasse, a new absorption peak of 2245 cm^{-1} ($\text{C}\equiv\text{N}$ stretching) was clearly observed in bagasse-AN, which confirms that AN has been grafted onto bagasse.⁸ Besides, the intensity of 3373 cm^{-1} for $-\text{OH}$ group became weaker due to the reaction of AN with hydroxyl of bagasse according to the synthesis chart in Figure 1. After the amination reaction of the bagasse-AN with DETA, the spectrum of the AB changes obviously. The broad absorption band for $-\text{OH}$ group is much stronger and a little red shift observed from 3373 cm^{-1} to 3353 cm^{-1} , which is probably due to the superposition of the a stretching vibrations of hydroxyl group and the N-H stretching vibrations of $-\text{NH}$ and $-\text{NH}_2$ groups,²⁵ the new peaks at 1643 cm^{-1} could be assigned to the stretching of $\text{C}=\text{N}$ in amide groups, which was not observed in the bagasse-AN. Besides, the absorption peak of 2250 cm^{-1} for nitrile group disappeared. These results indicate that $\text{C}\equiv\text{N}$ of AN has been aminated and DETA was grafted onto the bagasse-AN. In addition, the intensity of the adsorption band of 1057 cm^{-1} for $\gamma_{\text{C-O}}$ was slightly decreased due to the degradation of cellulose during dissolution and amination.

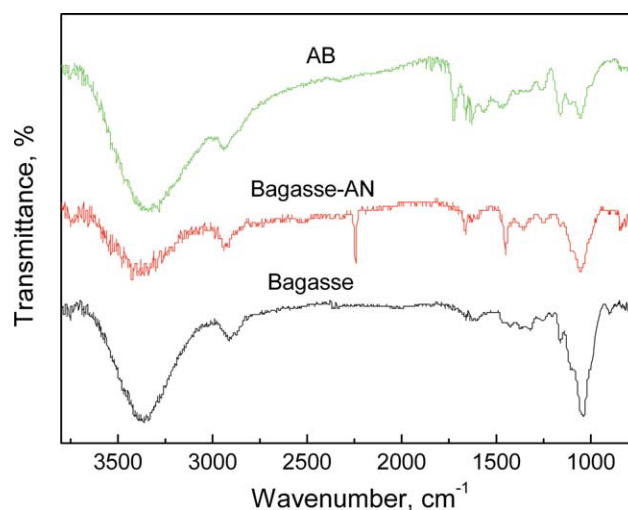


Figure 4 FTIR spectra of bagasse, bagasse-AN, and AB. [Color figure can be viewed in the online issue, which is available at www.interscience.wiley.com.]

Thermal properties of the AB

The TGA thermogram of bagasse and AB are presented in Figure 5. The thermal analysis of the bagasse showed that there was a mass loss from lower temperatures up to 480°C . The original bagasse was converted into CO_2 and H_2O completely and sharply at around 380°C . Besides, there is only one platform in the decomposition process of original bagasse. In the case of AB, it is roughly seen that there are two stages of mass loss and the starting decomposition temperature are at 120°C and 360°C , respectively. Although the starting decomposition temperature of bagasse-AN decreased, the degradation process was delayed. It is believed that the first platform comes from the loss of water vapor and the later

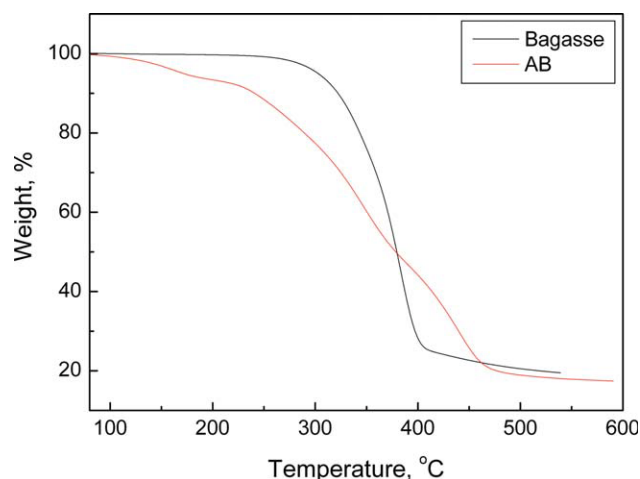


Figure 5 TGA thermograms of the bagasse and AB. [Color figure can be viewed in the online issue, which is available at www.interscience.wiley.com.]

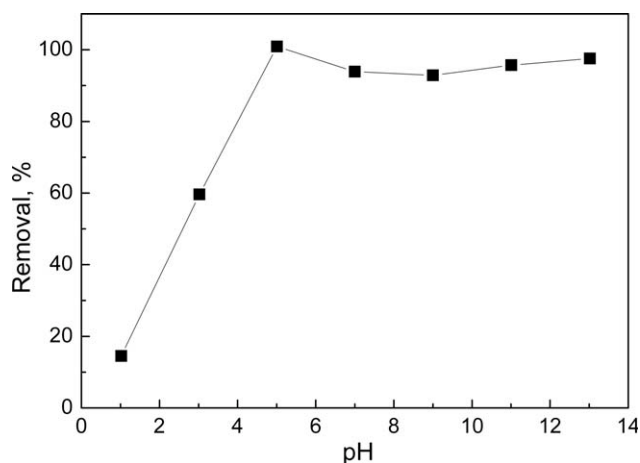


Figure 6 Effect of pH on the removal efficiency of AB for mercury ions.

corresponds to organic matter decomposition as well as to volatile substance.²⁵

Batch adsorption

Effect of pH on adsorption

Many researchers have verified that pH value of solution possess a significant influence on the adsorption of metal ions, as pH can affect the surface charge of an adsorbent, conformation of molecular structure, and stability of metal complexes.²⁶ To investigate the effect of pH on the adsorption performance of AB for mercury ions, equilibrium adsorption experiments were performed using an initial concentration of 100 mg/L over the pH range 1.0–13.0 and the results are shown in Figure 6.

It can be noted that the adsorption capacity for mercury ions rises dramatically with the pH increasing from pH 1 to 5 and reaches the highest adsorption capacity at pH 5, after that the higher removal percentage of mercury ions can be maintained for pH value of solution higher than 5. As well known, the protonation and deprotonation behaviors of acidic and basic groups would be influenced at different pH values. According to stability constant calculations, at lower pH values, HgCl_2 was the main species in the presence of chloride ions,^{27,28} and the hydrogen ions are adsorbed preferentially, occupying the active adsorbent sites, which lead to the adsorbent surface tends to present a positive charge.²⁵ The high hydrogen ion concentration at the interface repels the positively charged mercury ions electrostatically and prevents their approach to the bagasse surface. With pH increasing, the type of the species of mercury in solutions also changed and $\text{Hg}(\text{OH})_2$ is dominant at $\text{pH} > 4.0$,²⁹ while the degree of protonation of surface gradually reduced, less competition from protons and increase in concentration of

$\text{Hg}(\text{OH})_2$ species together lead to an increase in the removal efficiency for mercury.³⁰ Higher adsorption capacity at higher pH values is consistent with the stability of transition metal-amine complexes at higher pH values, which may imply that the adsorption mechanism is mainly chelating interactions between mercury ions and adsorbents.⁷ The results reveal that AB is effective for the removal of mercury over a wide range of pH, and the most suitable pH value is 5.0, so the further adsorption experiments were carried out at pH 5.

It is of concern if the mercury precipitates at a higher pH range when $\text{Hg}(\text{OH})_2$ is dominated, Zhang had done the solubility of $\text{Hg}(\text{II})$ versus solution pH in the absence of the adsorbent, and found that no significant change of dissolved $\text{Hg}(\text{II})$ at pH range of 1–12 at a initial concentration of $< 120 \text{ mg/L}$,⁵ which is implying that $\text{Hg}(\text{OH})_2$ is still dissolved in the solution when $\text{Hg}(\text{II})$ concentration is not too high.

Adsorption kinetics

The dynamic adsorption results of the AB for mercury are presented in Figure 7, which shows the tendency of adsorption amounts of mercury on the AB versus adsorption time. It can be seen that mercury removed by the AB increased sharply with the increasing of adsorption time and achieved higher than 80% of removal efficiency in 2 h. However, it needs 24 more hours to attained adsorption equilibrium. Besides, the equilibrium time is independent on the initial mercury concentration.

Adsorption isotherms

The equilibrium adsorption isotherm of three different grafting degrees AB (26.2%, 35.0%, and 58.3%) for

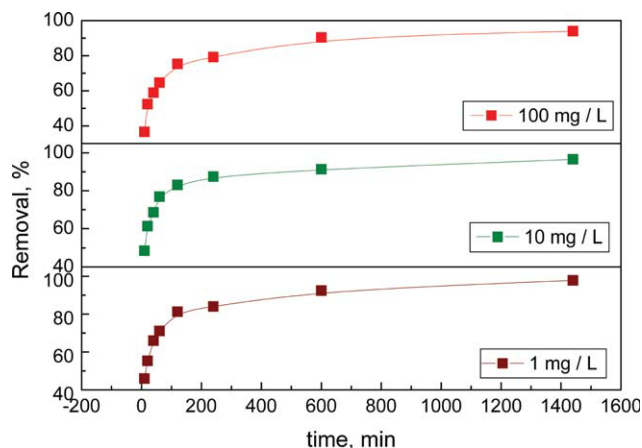


Figure 7 Adsorption kinetics of mercury on AB for different initial concentrations. [Color figure can be viewed in the online issue, which is available at www.interscience.wiley.com.]

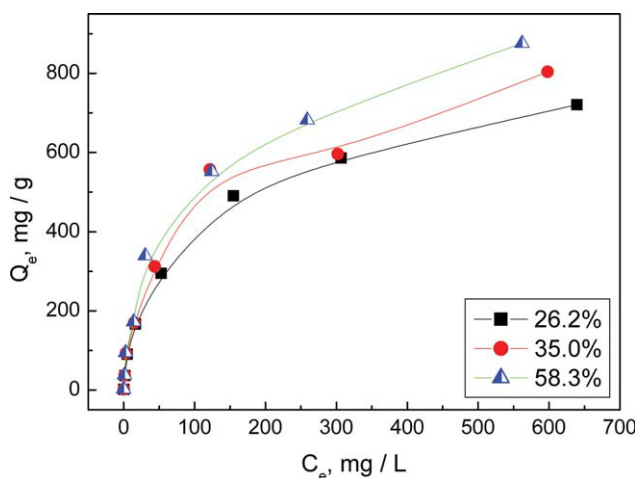


Figure 8 Effect of initial concentration on the removal efficiency of AB for mercury ions. [Color figure can be viewed in the online issue, which is available at www.interscience.wiley.com.]

mercury ions were investigated over a range of initial mercury concentrations. The results are shown in Figure 8. It is evident that an increase in the initial mercury concentration leads to a larger adsorption amount for mercury ions and a higher residual concentration at equilibrium, and then the uptake reaches a plateau at higher concentration, which resulted from the saturation adsorption of mercury ions on the chelating sites of the AB. In addition, the results illustrate that the adsorption capacity of AB increases with grafting degree of bagasse-AN. Most importantly, the adsorption capacity could be as high as 917.4 mg/g for mercury, which highlighting its potential application in wastewater treatment of large scale.

The experimental adsorption capacities, calculated by Langmuir equations basing on the experimental isotherms presented in Figure 8, are 769.2, 833.3, and 917.4 mg/g, respectively. And those of theoretical values were calculated according to the nitrogen content by elemental analysis (EA), basing on two amine chelating with one mercury ion.³¹ And element analysis shows the nitrogen percentages of the three different grafting degrees AB are 10.73, 11.35, and 13.31%, respectively, so theoretical adsorption capacity are 766.4, 810.7, and 950.7 mg/g, respectively. It can be noticed that the adsorption capacity of the three different grafting degrees AB are very close to those of theoretical values, so it can be speculated that the adsorption mechanism is dominated by chelating adsorption of nitrogen-containing functional groups with mercury ions.

Equilibrium data were fitted with two commonly used equilibrium models, Langmuir adsorption equation [eq. (3)] and Freundlich isotherm [eq. (4)], to evaluate which best fits the experimental data. They can be expressed as:³²

$$Q_e = \frac{Q_m C_e}{1/b + C_e} \tag{3}$$

$$Q_e = K_F C_e^{1/n} \tag{4}$$

where Q_e is the amount of mercury ions adsorbed onto the AB at equilibrium, Q_m is the maximum amount of adsorption (mg/g), b is the adsorption equilibrium experimental constant (1/mg), K_F ($L^n \text{ mg}^{1-n}/\text{g}$) and n are the Freundlich constants denoting adsorption capacity and intensity of adsorption, respectively, C_e is the mercury concentration (mg/L) in the solution at equilibrium, and Q_e and b are related to adsorption capacity and energy of adsorption, respectively.

The fitting results for Langmuir and Freundlich are shown in Figures 9 and 10, respectively. In the present study, the Langmuir model fitted the data slightly better than the Freundlich model, as evidenced by a higher R^2 in Langmuir model. The Langmuir isotherm derived from simple mass action kinetics is based on the assumptions that molecules are adsorbed as a saturated monolayer of one molecule thickness with no transmigration in the plane of the surface, and interaction between adsorbed molecules are negligible with energy of adsorption remaining constant.²⁶ The linear plot in Figure 9 shows that the adsorption of mercury on AB follows Langmuir isotherm model, which indicates monolayer coverage of mercury on the AB surface, a typical adsorption behavior of most metal ions. From the Langmuir equation, the maximum adsorption capacities of these AB for mercury were calculated to be 769.2 mg/g, 833.3

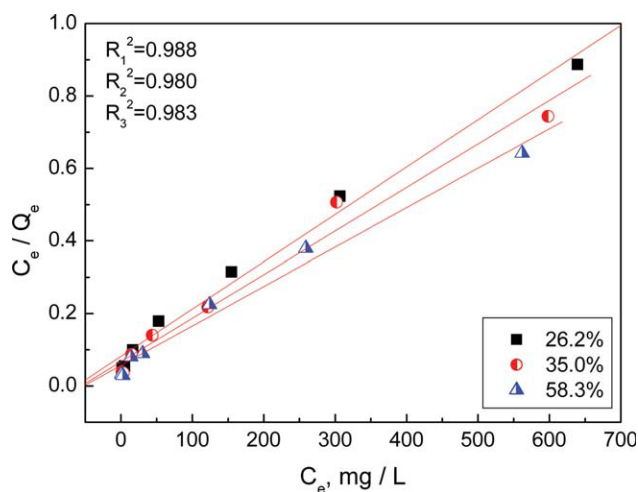


Figure 9 Linear fitting using Langmuir equation for the adsorption of mercury on AB. [Color figure can be viewed in the online issue, which is available at www.interscience.wiley.com.]

mg/g, and 917.4 mg/g for the grafting degree of 26.2, 35.0, and 58.3%, respectively.

Reusability

To apply adsorbents to real wastewater, the mercury desorption behavior were examined using a series of desorption solution. It was found that mercury desorption was 69.7, 81.1, 82.9, 87.3, and 86.5% with 1M HCl, 5M HCl, 3M HCl + 0.5%CS(NH₂)₂, 3M HCl + 2%CS(NH₂)₂, and 5M HNO₃, respectively. The highest desorption percentage was obtained when CS(NH₂)₂ added into the desorption solution, since is known as a very strong chelating agent for mercury ions and was thought to make complex with mercury ions to replace the amine groups complexed with mercury ions. In addition, HCl and HNO₃ are both capable of desorption for mercury, and higher concentration of acid is beneficial to improve the desorption efficiency, which may be due to the formation of complexes with mercury ions and the crowding-out effect of a large amount of protons. To test the suitability and stability of the adsorbent, it was subjected to successive adsorption and desorption cycles with 3M HCl + 0.5% CS(NH₂)₂ as the desorbing agent and the results are shown in Figure 11. The adsorption capacity of recycled AB still can reach the level of 96% after four cycles, while the recovery of mercury almost maintained the level of around 85%. At the end of four cycles, the recovery and removal were a little decreased. Besides, the environmental requirements are also met by using nonhazardous chemicals on recycling adsorbent material. These results indicate that the AB could be used economically in actual process.

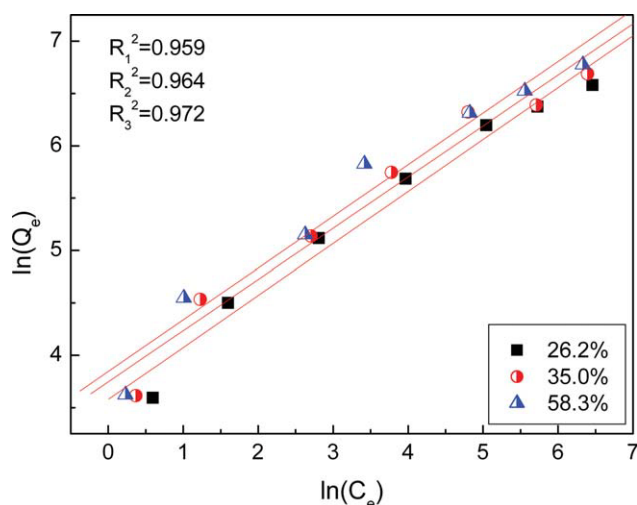


Figure 10 Linear fitting using Freundlich isotherm for the adsorption of mercury on AB. [Color figure can be viewed in the online issue, which is available at www.interscience.wiley.com.]

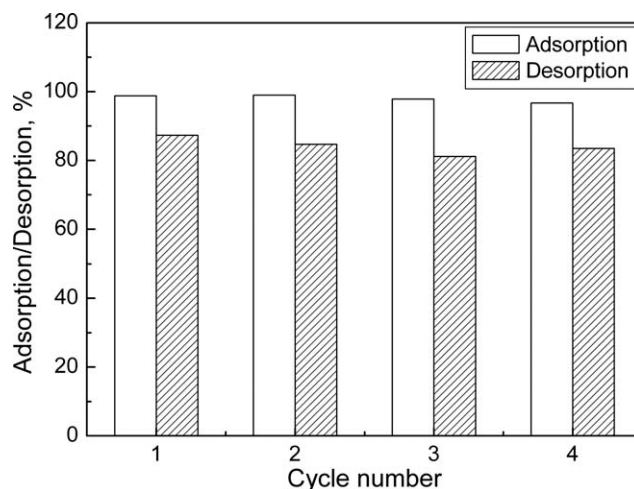


Figure 11 Four cycles of mercury adsorption-desorption with 3M HCl + 0.5% CS(NH₂)₂ as the desorption agent.

CONCLUSION

Through irradiation grafting modification, an AB containing chelating group of amine and amide was prepared. The AB is a suitable and effective adsorbent for the removal of mercury ions from aqueous solution. The optimized grafting conditions for irradiating dosage, concentration of AN (v/v) % and solvents are 48 KGy, 35% and DMF. The AB shows much higher adsorption capacities for mercury owing to its high-nitrogen percent and the strong affinity of the amine groups for mercury when pH value is more than 5, and the maximum adsorption capacity for mercury based on the Langmuir model is as high as 917.3 mg/g. In addition, the higher grafting degree of bagasse-AN, the higher adsorption capacity of AB for mercury ions, which is obviously due to the higher nitrogen percentage in higher grafting degree of AB. The results indicate that the great application potential of the AB in removal of mercury for effluent wastewater treatment.

References

- Garg, U. K.; Kaur, M. P.; Garg, V. K.; Sud, D. *Bioresour Technol* 2008, 99, 1325.
- Wan Ngah, W. S.; Hanafiah, M. A. K. M. *Bioresour Technol* 2008, 99, 3935.
- Nam, K. H.; Gomez-Salazar, S.; Tavlarides, L. L. *Ind Eng Chem Res* 2003, 42, 1955.
- Vieira, R. S.; Beppu, M. M. *Water Res* 2006, 40, 1726.
- Zhang, F.; Nriagu, J. O.; Itoh, H. *Water Res* 2005, 39, 389.
- Ritter, J. A.; Bibler, J. P. *Water Sci Technol* 1992, 25, 165.
- Herrero, R.; Lodeiro, P.; Rey-Castro, C.; Vilarino, T.; Sastre de Vicente, M. E. *Water Res* 2005, 39, 3199.
- Anirudhan, T. S.; Senan, P.; Unnithan, M. R. *Sep Sci Technol* 2007, 52, 512.
- Manohar, D. M.; Anoop Krishnan, K.; Anirudhan, T. S. *Water Res* 2002, 36, 1609.
- Jeon, C.; Park, K. H. *Water Res* 2005, 39, 3938.
- Karnitz, O. Jr.; Gurgel, L. V. A.; Freitas, R. P.; Gil, L. F. *Carbohydr Polym* 2009, 77, 643.

12. Gurgel, L. V. A.; de Freitas, R. P.; Gil, L. F. *Carbohydr Polym* 2008, 74, 922.
13. Liu, C.; Sun, R.; Qin, M.; Zhang, A.; Ren, J.; Xu, F.; Ye, J.; Wu, S. *Ind Crop Prod* 2007, 26, 212.
14. Srivastava, V. C.; Mall, I. D.; Mishra, I. M. *Chem Eng J* 2007, 132, 267.
15. Krishnan, K. A.; Anirudhan, T. S. *J Hazard Mater* 2002, 92, 161.
16. Jiang, Y.; Pang, H.; Liao, B. *J Hazard Mater* 2009, 164, 1.
17. Karnitz, O., Jr.; Gurgel, L. V. A.; de Melo, J. C. P.; Botaro, V. R.; Melo, T. M. S.; de Freitas Gil, R. P.; Frédéric Gil, L. *Bioresour Technol* 2007, 98, 1291.
18. Sousa, F. W.; Sousa, M. J.; Oliveira, I. R. N.; Oliveira, A. G.; Cavalcante, R. M.; Fechine, P. B. A.; Neto, V. O. S.; Keukeleire, D.; Nascimento, R. F. *J Environ Manage* 2009, 90, 3340.
19. Liu, C.; Sun, R.; Qin, M.; Zhang, A.; Ren, J.; Ye, J.; Luo, W.; Chao, Z. *Bioresour Technol* 2008, 99, 1465.
20. Yoshitake, H.; Yokoi, T.; Tatsumi, T. *Chem Mater* 2002, 14, 4603.
21. Baba, Y.; Ohe, K.; Kawasaki, Y.; Kolev, S. D. *React Funct Polym* 2006, 66, 1158.
22. Liu, C.; Sun, R.; Zhang, A.; Ren, J.; Wang, X.; Qin, M.; Chao, Z.; Luo, W. *Carbohydr Res* 2007, 342, 919.
23. Odian, G.; Sobel, M.; Rossi, A.; Klein, R.; Acker, T. *J Polym Sci Part A: Gen Pap* 1963, 1, 639.
24. Gurgel, L. V. A.; Gil, L. F. *Water Res* 2009, 43, 4479.
25. Farinella, N. V.; Matos, G. D.; Arrud, M. A. Z. *Bioresour Technol* 2007, 98, 1940.
26. Inbaraj, B. S.; Wang, J. S.; Lu, J. F.; Siao, F. Y.; Chen, B. H. *Bioresour Technol* 2009, 100, 200.
27. Budinova, T.; Petrov, J.; Parra, N.; Baloutzov, V. *J Environ Manage* 2008, 88, 165.
28. Rio, S.; Delebarre, A. *Fuel* 2003, 82, 153.
29. Say, R.; Birlık, E.; Erdemgil, Z.; Denizli, A.; Ersoz, A. J. *Hazard Mater* 2008, 150, 560.
30. Anirudhan, T. S.; Divya, L.; Ramachandran, M. *J Hazard Mater* 2008, 157, 620.
31. Ma, N.; Yang, Y.; Chen, S.; Zhang, Q. *J Hazard Mater* 2009, 171, 288.
32. Garg, U.; Kaur, M. P.; Jawa, G. K.; Sud, D.; Garg, V. K. *J Hazard Mater* 2008, 154, 1149.